Separation Science and Technology
Publication details, including instructions for authors and subscription information:
http://www.informaworld.com/smpp/title~content=t713708471

Separation of Argon and Oxygen by Adsorption on a Titanosilicate Molecular Sieve

Alejandro Ansón[a]; Steven M. Kuznicki[a]; Tetyana Kuznicki[a]; Brian C. Dunn[b]; Edward M. Eyring[b]; Douglas B. Hunter[c]
[a] Department of Chemical and Materials Engineering, University of Alberta, Edmonton, AB, Canada [b] Department of Chemistry, University of Utah, Salt Lake City, UT, USA [c] Savannah River National Laboratory, Aiken, SC, USA

To cite this Article Ansón, Alejandro , Kuznicki, Steven M. , Kuznicki, Tetyana , Dunn, Brian C. , Eyring, Edward M. and Hunter, Douglas B.(2009) 'Separation of Argon and Oxygen by Adsorption on a Titanosilicate Molecular Sieve', Separation Science and Technology, 44: 7, 1604 — 1620
To link to this Article: DOI: 10.1080/01496390902775315
URL: http://dx.doi.org/10.1080/01496390902775315

Separation Science and Technology, 44: 1604–1620, 2009

ISSN: 0149-6395 print/1520-5754 online
DOI: 10.1080/01496390902775315

Taylor & Francis
Taylor & Francis Group

Separation of Argon and Oxygen by Adsorption on a Titanosilicate Molecular Sieve

Alejandro Ansón,[1] Steven M. Kuznicki,[1] Tetyana Kuznicki,[1] Brian C. Dunn,[2] Edward M. Eyring,[2] and Douglas B. Hunter[3]
[1]Department of Chemical and Materials Engineering, University of Alberta, Edmonton, AB, Canada
[2]Department of Chemistry, University of Utah, Salt Lake City, UT, USA
[3]Savannah River National Laboratory, Aiken, SC, USA

Abstract: A titanosilicate molecular sieve adsorbent, Ba-RPZ-3, was synthesized and tested for its use in the separation of O_2+Ar mixtures at room temperature. A clean resolution of both gases was achieved in pulse chromatographic experiments using a standard column (0.25″ OD, 3.5 grams of adsorbent). In another experiment, using a column containing 30 grams of adsorbent and a continuous O_2+Ar feed at 10 cm^3/min, argon breakthrough was detected more than 5 minutes before the oxygen breakthrough, and the separation was sufficiently sensitive to achieve quantitative separation of mixtures with low argon content (5% Ar). Equilibrium adsorption isotherms and isosteric heats of adsorption for oxygen and argon were found to be almost identical at room temperature. The thermodynamic selectivity was found to be mildly in favor of oxygen (~1.1–1.2). However, the adsorption of oxygen was observed to be much faster than argon, indicating that the separation of the O_2+Ar mixtures was based on the sieving properties of the adsorbent and the difference in sizes of O_2 molecules and Ar atoms. This indicates that a suitably-oriented oxygen is physically smaller than argon, despite the fact that many references assume that oxygen is larger than argon.

Keywords: Air, argon, molecular sieve, oxygen, zeolite

Received 1 April 2008; accepted 8 January 2009.
Address correspondence to Steven M. Kuznicki, Department of Chemical and Materials Engineering, University of Alberta, Edmonton, AB T6G 2G6, Canada. Tel.: (780) 492-8819; Fax: (780) 492-8958. E-mail: steve.kuznicki@ualberta.ca

INTRODUCTION

The separation of argon and oxygen is one of the most important processes in the industrial purification of the constituents of air, and it is also one of the most difficult. The production of pure oxygen for industrial and medical applications requires the separation of oxygen and argon, two major constituents of air with very similar physical properties, including size and boiling point. The basic methods used to effect this separation include selective adsorption and cryogenic distillation. At cryogenic temperatures, the adsorptive selectivity of oxygen over argon on classical zeolites appears to be large enough for practical separation. Barrer and Robins (1) investigating the ability of sodium mordenite to separate several binary gas mixtures concluded that zeolite columns at −183°C can generate pure argon from O_2+Ar mixtures. They had previously detected wide differences in the sorption rates of the pure gases, hydrogen, neon, oxygen, nitrogen, argon, and krypton, and they attributed the resolution of the mixtures to both the affinity of the gases for the substrate and the sorption kinetics. In the case of O_2+Ar mixtures at low temperature, both factors tend to maximize the preferential sorption of oxygen over argon. The chromatographic resolution of argon and oxygen can also be achieved in a column of zeolite 5A at dry ice/acetone bath temperatures (−78°C) (2). Chromatographic systems including cryogenic columns for the separation of argon and oxygen have been utilized to solve practical analytical problems (3,4). Such separations of argon and oxygen on zeolites at cryogenic temperatures could be implemented as industrial processes (5), if they did not have high energy requirements.

Unfortunately, at room temperature little or no selectivity for O_2 over Ar is found for common adsorbents, including zeolites. Isosteric heats of adsorption for argon and oxygen are generally nearly identical, the only exception being silver exchanged molecular sieves, which are reported to show mild argon selectivity (1.2–1.5) (6). Attempts to exploit the mild thermodynamic selectivity for oxygen over argon by the chromatographic separation of oxygen and argon using columns containing 5A zeolite (7), 13X zeolite (8), or Ca chabazite (one of the most polarizing adsorbents known) (9), have been made, but all require extremely dry adsorbents and commercially impractical processes with very low product yield. The use of very long chromatographic columns (several meters) of porous polymers (10,11) to effect this separation has also been reported.

Early attempts to separate O_2+Ar mixtures by selective adsorption at ambient temperature were done using chromatographic columns of zeolites and polymers. More recently, bulk industrial processes involving

carbon molecular sieves have been proposed, both for the purification of oxygen from O_2+Ar mixtures and to obtain an argon enriched stream (12,13). The thermodynamic selectivity of oxygen in carbon molecular sieves is too small to allow equilibrium-based pressure swing adsorption cycles, but the sorption of oxygen is much faster than the rate of argon (25 or 30 times), opening the possibility of pressure swing adsorption (PSA) processes based on kinetic selectivity (12–14). It is believed that the size of the gas molecules plays the main role in determining adsorption kinetics (15,16). The separation of oxygen and argon with carbon molecular sieves (CMS) is far from perfect, in fact, the maximum argon purity reported for this process using CMS is on the order of 80–90% (12,13). In a model calculation of a 5-step cycle designed for producing high purity argon using a Berghan-Forschung activated carbon at 30°C, the highest projected argon purity was 88% but that allowed the recovery of only 15% of the argon of the original stream (12). Calculations for a 3-step PSA cycle using a Takeda carbon molecular sieve at 20°C projected a maximum argon purity of about 80% with recovery of 43% (13). This report concluded that the Takeda molecular sieve carbon was better for this separation than either a Berghan-Forschung activated carbon or a modified 4A zeolite (RS-10). An inorganic molecular sieve with cleaner resolution of oxygen and argon and better predictability than current CMS materials could enable more efficient processes for oxygen and argon separation and purification.

Several titanosilicates, including ETS-4 (17–19), ETS-10 (20), and other structures based on octahedral titanium units (21,22), have been recognized for their adsorptive and molecular sieving properties. ETS-4, in particular, has been noted for its ability to differentiate molecules by size, including the commercial separation of N_2 from methane at high pressure (17–19). In the present report, we examine the separation of O_2 and Ar using Ba-RPZ-3, a new, zorite-like member of the titanosilicate family (23–25).

RPZ-3 (reduced pore zorite) (26) is a structural analog of the mineral zorite and the synthetic titanosilicate ETS-4. RPZ-3 contains structural chloride ions which constrict the pore progressively and systematically as their concentration increases. This new method of pore size control allows size-selective materials to be prepared in stable forms without crystal shrinkage. This allows the preparation of even more precise size exclusion adsorbents than the "Molecular Gate"® (19) effect noted for other titanosilicate molecular sieves.

In this work, O_2+Ar mixtures were separated using Ba-RPZ-3. Chromatographic resolution was evaluated for O_2+Ar mixtures initially containing as little as 5% argon, which is the typical outlet stream in primary PSA air separation processes. Based on the results of these

separations, the sieving characteristics of this material were considered in terms of a kinetic mechanism selective toward the sorption of O_2.

EXPERIMENTAL

RPZ-3 was synthesized by thoroughly mixing 25.1 g of N-Brand sodium silicate (29% SiO_2, 9% Na_2O), 4.6 g of NaOH and 16.3 g $TiCl_3$ (Fisher, 20%) with 3.0 g of potassium chloride (Fisher). The mixture was stirred for one hour, then transferred into, and reacted in a sealed autoclave (PARR Instruments) at 200°C for 48 h. The resultant product was thoroughly washed with de-ionized water, and dried in a forced-air oven at 80°C. The as-synthesized RPZ-3 was barium exchanged by exposure to an excess of aqueous solution of barium chloride at 100°C with stirring for 24 hours. Sodium is essentially quantitatively exchanged by barium with the finished material typically containing nearly 30 wt% barium and <1 wt% sodium. Barium is known to stabilize titanosilicate molecular sieves and maximum replacement of sodium is desired. The Ba-exchanged RPZ-3 was thoroughly washed with de-ionized water, and dried at 100°C. The average particle size produced for testing was approximately 40 μm.

For comparison, ETS-4 was synthesized (27) and barium exchanged as above.

The as-synthesized RPZ-3 was examined by X-ray powder diffraction analysis (XRD) using a Rigaku Geigerflex 2173 vertical goniometer equipped with a graphite monochromator for filtration of K-α wavelengths. Figure 1 depicts the XRD pattern of as synthesized RPZ-3. Peak positions are reminiscent of the mineral zorite (23–25) and its closest synthetic analog, ETS-4 (27), but with differing peak intensity ratios. It is clear that, like ETS-4 and its polymorphs (27), RPZ-3 is structurally related to the mineral zorite.

Inverse gas chromatography experiments were performed using a Varian 3800 Gas Chromatograph (GC) utilizing the thermal conductivity detector. Test adsorbents were packed into 10'' long, 0.25″ OD copper columns. The columns were filled with approximately 3.5 grams of adsorbent. The adsorbents were activated at 250°C for 10 h under a flow of 30 cm^3/min helium carrier gas. Pulse injections were performed using 1 mL of argon, oxygen, or mixtures thereof.

The ability of the titanosilicate molecular sieve to concentrate argon from an O_2+Ar mixture was further investigated using a continuous flow apparatus (Fig. 2). The unit consisted of a single adsorbent bed equipped with a gas chromatograph (GC) for the analysis of the outlet stream. The flow rate of each gas (helium, oxygen, and argon) was adjusted by mass

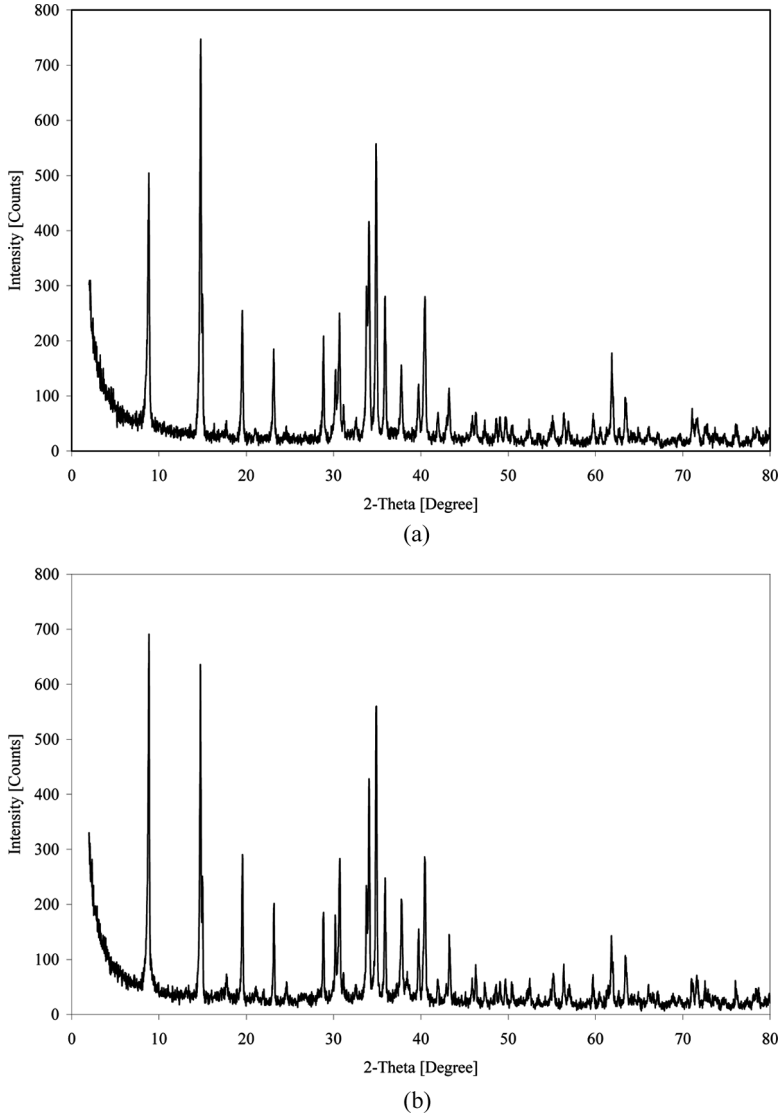

Figure 1. XRD pattern of (a) ETS-4 and (b) RPZ-3, the titanosilicate molecular sieve adsorbent studied in this work.

flow controllers (MFC). The experiments were conducted by first purging the bed with helium at a flow rate of 15 cm^3/min. The separation of argon and oxygen by adsorption on Ba-RPZ-3 was measured in a continuous flow system using both a 50–50% O_2+Ar mixture and a 95–5%

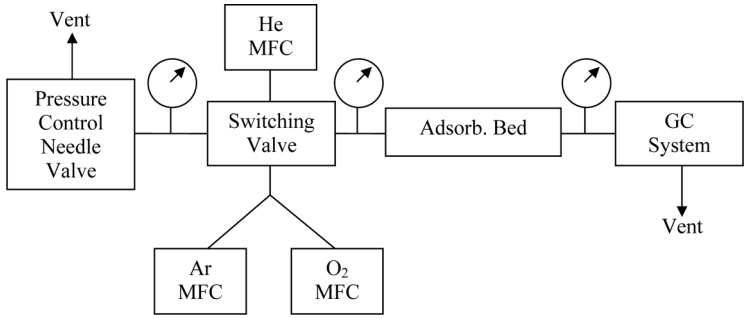

Figure 2. Block diagram of the laboratory scale PSA apparatus employed for the oxygen breakthrough determinations.

O_2+Ar mixture. The bed dimensions were 0.5″ OD and 17″ length. The chamber had a volume of 47 cm^3, and contained slightly more than 30 g of the adsorbent. The total flow rate through the bed was 10 cm^3/min, so for the 50–50% O_2+Ar mixture, the flows of each gas were 5 cm^3/min. Measurements were conducted with the bed at ambient temperature.

Oxygen and argon adsorption isotherms were measured at 25, 30, and 35°C in a Rubotherm magnetic suspension balance (accuracy $\pm 1\,\mu g$), integrated into a GHP high pressure adsorption system constructed by VTI Corp. of Hialeah, FL. Test samples were dried at 200°C for 6 hours under a vacuum of greater than 10^{-4} Torr. Buoyancy effects were corrected with helium displacement isotherms taken at the same temperatures.

Adsorption kinetics measurements were also performed in the Rubotherm system. Weight change vs time was measured in the pressure regimes of 40–70 and 70–100 kPa. Experimental conditions were identical to those used for collecting of the equilibrium isotherms.

RESULTS

Figure 3a illustrates the pulse chromatographic separation of 1 cm^3 of a 50–50% $O_2 + Ar$ mixture on the barium exchanged titanosilicate molecular sieve at 30°C. Compared to the pure gas chromatographic data (Figs. 3c and 3d), it is clear that the first peak represents Ar, while the second peak represents O_2. The same peak identification can be assigned to Fig. 3b, which illustrates the separation of 1 cm^3 of a 90–10% $O_2 + Ar$ mixture on the same column. Ba-RPZ-3 clearly demonstrates the clean resolution of O_2 from Ar under the experimental GC conditions. The argon and oxygen retention times (Fig. 3) are almost identical regardless

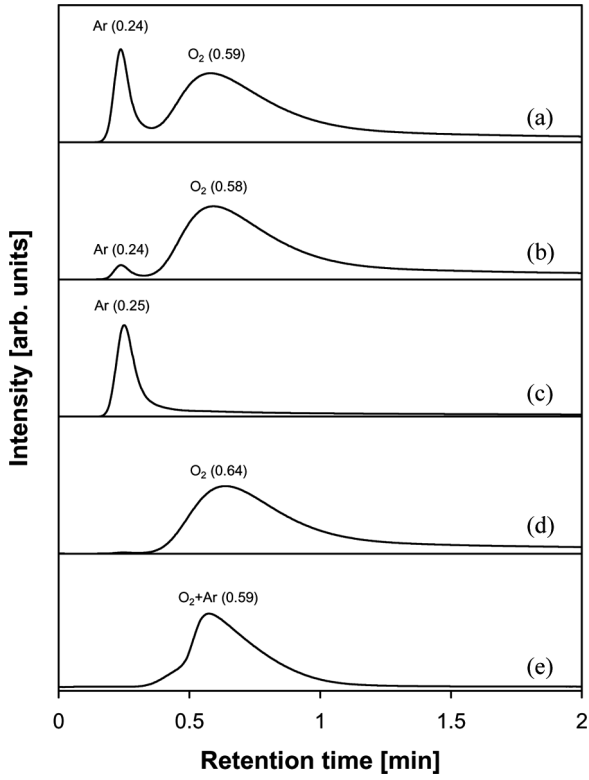

Figure 3. Chromatographic profiles at 30°C under 30 cm^3/min carrier gas helium obtained by injecting: (a) 50–50% $O_2 + Ar$; (b) 90–10% $O_2 + Ar$; (c) pure argon; (d) pure oxygen in a column of Ba-RPZ-3; and (e) 50–50% $O_2 + Ar$ in a column of Ba-ETS-4.

of the composition of the $O_2 + Ar$ mixture. For comparison, an identically sized column of barium exchanged ETS-4 was run with a 1 cm^3 injection of 50–50% $O_2 + Ar$ mixture and shows no resolution of these gases as seen in Fig. 3e.

The experimental results obtained from the continuous flow unit for a 50–50% $O_2 + Ar$ mixture are presented in Fig. 4 and for a 95–5% $O_2 + Ar$ mixture are presented in Fig. 5. Figures 4a and 5a show the GC peak intensities normalized to the equilibrium values for oxygen and argon in the exit stream as a function of time. The normalized signal area (the area under the band signal in the normalized profile) is greater than unity at some times because of the fixed volume injection. When only argon was exiting the adsorbent bed (prior to oxygen breakthrough),

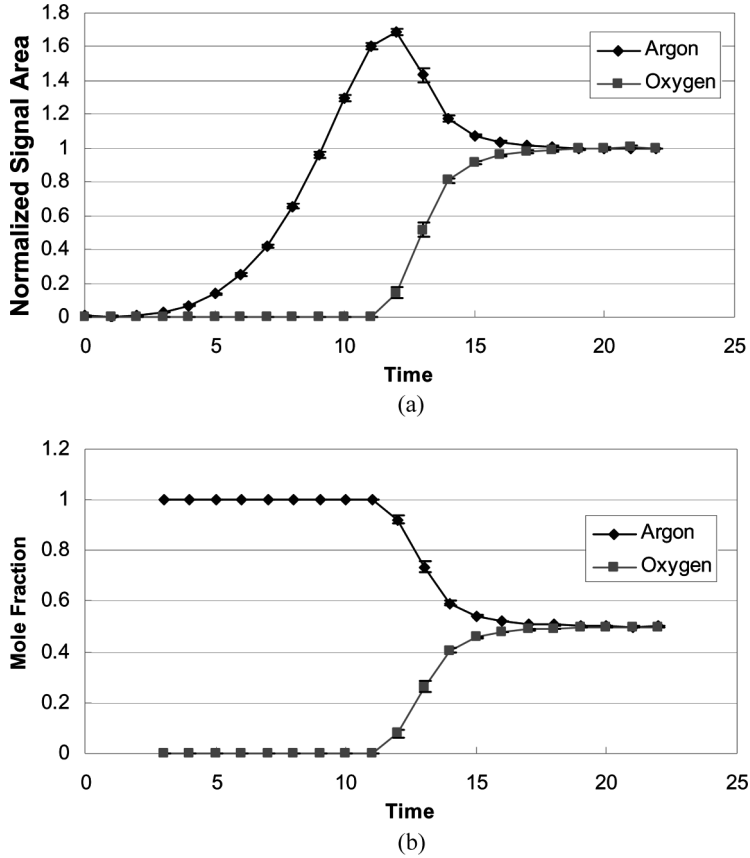

Figure 4. GC analysis at the outlet stream of the Ba-RPZ-3 adsorbent bed after switching a continuous flow of 50–50% $O_2 + Ar$ inlet mixture: (a) variation of the GC normalized peak areas (for argon and oxygen), and (b) changes in the argon and oxygen mole fractions as a function of time (minutes).

the concentration of argon in the injection volume was significantly larger than the equilibrium concentration. Figures 4b and 5b depict the relative argon and oxygen mole fractions at the outlet of the adsorbent bed. All data points in Figs. 4 and 5 represent the mean values of triplicate GC analysis and the error bars depicted represent the standard deviation of the three runs.

For the 50–50% $O_2 + Ar$ mixture (Fig. 4), oxygen was not detected at the outlet until the mixture had flowed for 8 minutes (the 4 minute offset is due to the analysis time). Only argon was noted in the product stream until the oxygen breakthrough at 8 minutes. For the 95–5% $O_2 + Ar$

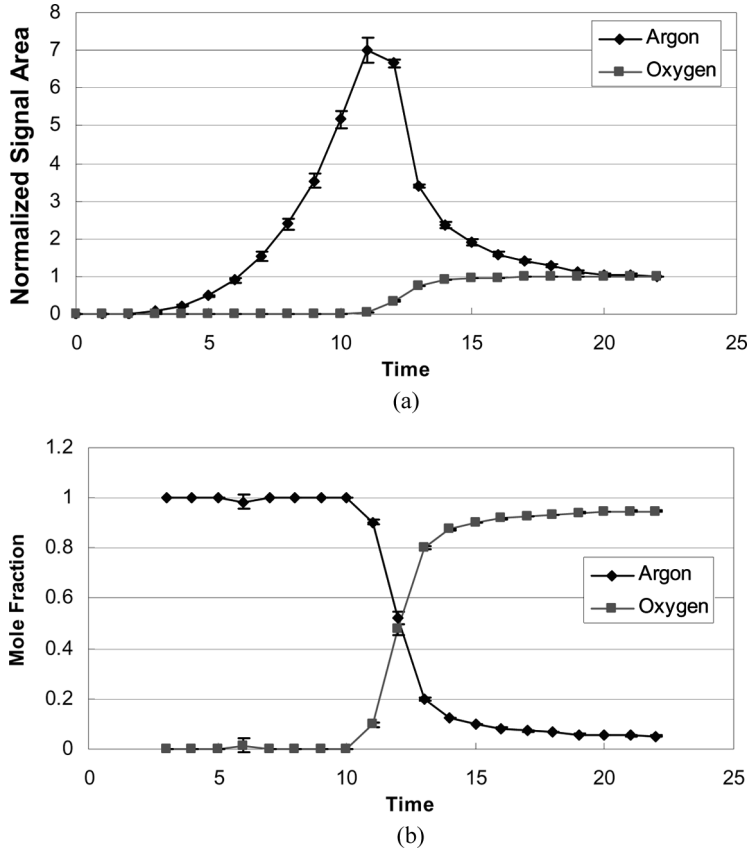

Figure 5. GC analysis at the outlet stream of Ba-RPZ-3 adsorbent bed after switching a continuous flow of 95–5% $O_2 + Ar$ inlet mixture: (a) variation of the GC normalized peak areas (for argon and oxygen), and (b) changes in the argon and oxygen mole fractions as a function of time (minutes).

mixture (Fig. 5), the oxygen did not begin to appear in the output stream until 7 minutes after the flow had been initiated.

Figure 6 shows the oxygen and argon equilibrium adsorption isotherms at 30°C for the Ba-RPZ-3 adsorbent. The total adsorption capacities for oxygen and argon are similar. At 25, 30, and 35°C, argon and oxygen isotherms in the range of 1–200 kPa can be described well by the classical Langmuir equation:

$$n = \frac{n_m \cdot K_L \cdot p}{1 + K_L \cdot p},$$

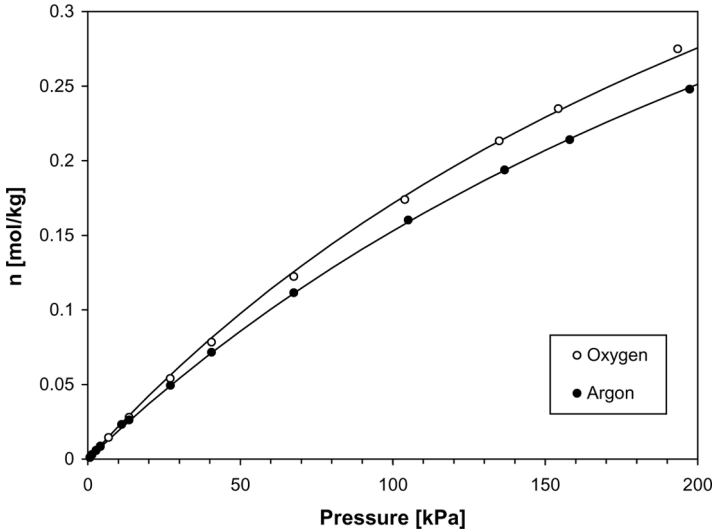

Figure 6. Oxygen and argon equilibrium adsorption isotherms at 30°C for Ba-RPZ-3.

where n is the adsorbate concentration [mol/kg] at the pressure p [kPa], and K_L and n_m are fitting parameters. The product $K_L \cdot n_m$ equals the Henry's law constant (K), observed at the low pressure linear region of the isotherm. After calculating the parameters K_L and n_m for the entire set of isotherms, the value of the monolayer capacity was evaluated by averaging the parameters n_m. Then, the isotherms were fitted again, restricting n_m to the averaged number (0.70 mol/kg). The values of $K_L \cdot n_m$ obtained in this way are listed in Table 1, together with the estimated standard deviation (SD) for the fittings:

$$SD = \sqrt{\frac{\sum (n_{exp} - n_{calc})^2}{N - 2}},$$

where n_{exp} is the experimental adsorbate concentration at a pressure p, n_{calc} is the adsorbate concentration calculated from the Langmuir equation at the same pressure, and N is the number of experimental points.

The thermodynamic selectivity of oxygen over argon can be calculated as the ratio of the respective Henry's law constants. According to the values listed in Table 1, the thermodynamic selectivity of oxygen (over argon) is 1.17, 1.16, and 1.14 at 25, 30, and 35°C respectively.

Table 1. Equilibrium and kinetic parameters for the adsorption of oxygen and argon on Ba-RPZ-3: Henry's law constant (K), standard deviation (SD) for the Langmuir isotherm fitting, and diffusion coefficients (D/r^2)

				$10^3 \cdot D/r^2$ [s^{-1}]	
	T [°C]	$10^3 \cdot K$ [mol/kg·kPa][a]	$10^3 \cdot SD$	40–70 kPa	70–100 kPa
Oxygen	25.5	2.542	2.1	2.129	2.502
	30.3	2.266	2.4	2.569	2.436
	35.2	1.903	0.9	2.250	2.398
Argon	25.5	2.164	2.2	0.280	0.346
	30.2	1.955	0.9	0.319	0.400
	35.2	1.670	1.8	0.424	0.502

[a]the value obtained for the monolayer capacity in the Langmuir equation was $n_m = 0.7031$ mol/kg.

The Henry's law constants were also used to estimate the limiting isosteric heats of adsorption by means of the van't Hoff isobar. The heat of adsorption for oxygen (22.8 kJ/mol) is only slightly higher than that for argon (20.5 kJ/mol). The heats of adsorption for argon and oxygen on Ba-RPZ-3 are slightly higher than those reported for a carbon molecular sieve commercialized by Air Products and Chemicals Inc. (18.6 ± 0.4 and 18.3 ± 0.7 kJ/mol for oxygen and argon, respectively) (15). With such similar values for thermodynamic selectivity and heats of adsorption, the separation of argon and oxygen observed for Ba-RPZ-3 in the chromatographic experiments cannot be explained in terms of equilibrium parameters.

However, a substantial difference is observed in the rate of adsorption of oxygen and argon on Ba-RPZ-3. As is shown in the uptake curves of Fig. 7 (fractional uptake vs. time), equilibrium capacity is achieved much faster in the case of oxygen than argon. The fractional uptake in Fig. 7 is defined as $(w_t - w_o)/(w_{eq} - w_o)$, where w_o is the adsorbate loading at the beginning of the pressure step (time = 0), w_t is the adsorbate loading at time t (sec), and w_{eq} is the adsorbate loading in equilibrium at the end of the pressure step. The kinetic experimental data were fitted to an expression describing the diffusion of gases inside zeolite channels (13):

$$\frac{w_t}{w_{eq}} = 1 - \frac{6}{\pi} \sum_{n=1}^{\infty} \frac{\exp(-n^2 \pi^2 Dt/r^2)}{n^2},$$

where D/r^2 is the rate constant for the process. The values of D/r^2 were calculated by fitting the experimental data to the expression above for

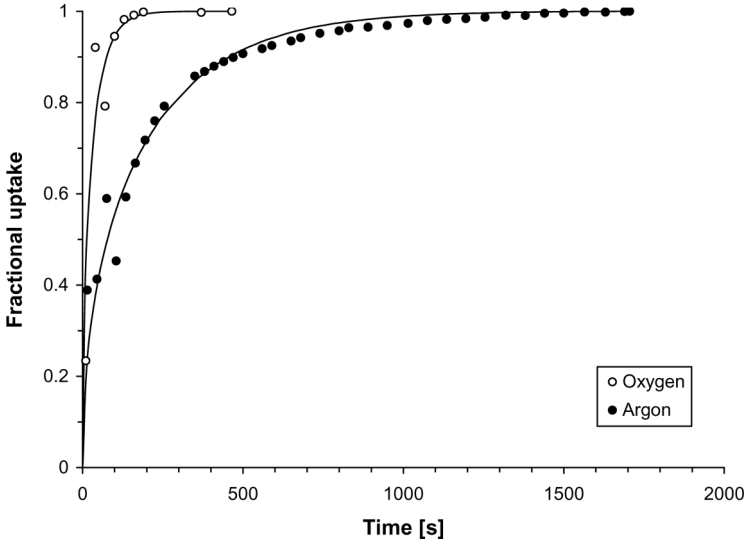

Figure 7. Adsorption uptake curves for oxygen and argon at 30°C in the pressure step 70–100 kPa.

oxygen and argon at 25, 30, and 35°C for the two pressure steps (40–70 and 70–100 kPa) that are listed in Table 1. The ratio of the diffusion rate constants for oxygen and argon are in the range of 5–8 under these conditions. The kinetic selectivity (α) of oxygen over argon can be calculated by applying the following expression (13):

$$\alpha = \frac{K_A}{K_B}\sqrt{\frac{D_A}{D_B}},$$

where K is the Henry's law constant as listed in Table 1, D is as defined above, and subscripts A and B refer to oxygen and argon. The kinetic selectivity to oxygen for Ba-RPZ-3 results to be in the range of 2.5–3.3. This represents the minimal value because of experimental limitations. The rate of argon uptake is reasonably well defined. But for oxygen, the beginning of the uptake curve is poorly defined because the gas adsorption is faster than the balance equilibration time. It is thus possible that values of D/r^2 determined are too small in the case of oxygen and the true kinetic selectivity vs. argon maybe somewhat higher. The energy associated to the diffusion of argon into the adsorbent can be calculated by applying the Arrhenius equation. This results in values of 32.0 and 28.8 kJ/mol in the pressure regimes of 40–70 and 70–100 kPa, respectively. This value is somewhat lower than that calculated for a carbon

molecular sieve commercialized by Air Products and Chemicals which was 41.4 ± 3.8 and 43.3 ± 2.9 kJ/mol for the pressure steps 30–50 and 50–100 kPa, respectively (15).

DISCUSSION

The present data clearly indicate that the separation of O_2+Ar mixtures is due to kinetics rather than thermodynamics which is likely associated with the molecular sieve effect. However, most reference works indicate that size difference between oxygen and argon lies between 0.06 and 0.08 Å which is too small to explain the observed molecular sieve effect.

The size of adsorbable gas molecules is usually assessed by the effective kinetic diameter of that gas. Since the suggested application to molecular sieves by Breck (28), the concept of effective kinetic diameter has become the most commonly accepted measure of gas particle sizes interacting with molecular sieve type adsorbents. Effective kinetic diameters have been reported by Hirschfelder et al. (29) as well as by Sircar and Myers (30). Their values for argon, nitrogen, and oxygen are listed in Table 2.

Generally, the effective kinetic diameter of a gas is defined by a Lennard-Jones 12–6 type function describing the potential energy of two interacting objects (φ(r)) as a function of their distance, measured by the separation of their nuclei (r)

$$\varphi(r) = 4\varepsilon\left[(\frac{\sigma}{r})^{12} - (\frac{\sigma}{r})^{6}\right].$$

The exponent of the attractive term expressed as the power of 6 of the function is well defined in theory, accounting for induced dipole–dipole

Table 2. Effective kinetic diameters and dimensions of argon, nitrogen, and oxygen

Gas	Effective kinetic diameter[a] [Å] (Breck's)	Effective kinetic diameter[b] [Å] (Sircar's)	MIN-1[c] [Å]	MIN-2[c] [Å]	3rd dimension[c] [Å]
Ar	3.40	3.542	3.510	3.630	–
N_2	3.64	3.64–3.80	2.991	3.054	4.046
O_2	3.46	3.467	2.930	2.985	4.052

[a]Page 636 (28).
[b]Pages 1068–1069 (30).
[c]Refs. 32 and 34.

interactions between objects. The exponent of the repulsive term expressed as the power of 12 must be chosen empirically. This semi-empirical function works well for gas–gas interactions, describing the behavior of a number of gases when no adsorbent is present.

The effective kinetic diameter of the interacting objects (σ), is the size parameter corresponding to zero potential energy, not the minimum of the potential energy, resulting from the interaction. The minimum of the potential energy, σ, is at r_{min}, expressed as

$$r_{min} = 2^{1/6}\sigma.$$

The factor $2^{1/6}$ is a strictly mathematical consequence of the Lennard-Jones 12–6 function chosen. The σ values can also be calculated from experimentally determined second virial coefficients (29).

The Lennard-Jones model depicts the atoms as soft spheres. If the interatomic distance is smaller than σ, the potential energy increases steeply. The adsorbent framework is not a rigid structure. Molecular sieve frameworks are held together by strong, covalent bonds, and these bonds vibrate. The atom-to-atom distances and the bond angles can change with the external conditions, and also adjust in the presence of an adsorbent (31). Therefore, the effective kinetic diameter of a molecule is not an absolute universal size parameter for gas-adsorbent interactions under all conditions.

An alternative approach to the kinetic diameter was proposed by Webster et al. (32,33) to address the problem of interaction between an adsorbate and a crystalline pore for non-spherical adsorbate molecules. This approach considers not only the size of the pore but its shape as well. Instead of a single size parameter, a set of parameters for each adsorbate is considered based on quantum chemistry and van der Waals sizes. The first size parameter, MIN-1 is the smallest cross section of the gas molecule. The second size parameter, MIN-2, is the next largest dimension of the gas molecule. MIN-1 and MIN-2 are chosen to be perpendicular.

The MIN-2 size parameter for Ar in Table 2 is reported as 3.63 Å, which is larger than the effective kinetic diameter. The MIN-2 values for O_2 and N_2 are both much smaller than their effective kinetic diameters. According to this model, the observed adsorption of O_2 is explained by the oriented interaction between the zeolite window and the O_2 molecule. Instead of a randomly oriented molecule, this model anticipates oxygen approaching the pore along the diatomic axis of the molecule (“head-on”), exposing a much smaller molecular cross section, than the effective kinetic diameter. Oxygen can pass through the window with this orientation. Eventually, many oxygen molecules interact with the window in this favored orientation. Argon, on the other hand, behaves as a solid sphere. Its orientation does not influence its apparent

size. Because of this, oxygen with a larger effective kinetic diameter actually enters the crystalline pores more rapidly than "smaller" argon.

CONCLUSIONS

A titanosilicate molecular sieve, Ba-RPZ-3, was shown to have the ability to cleanly resolve mixtures of oxygen and argon at room temperature. This separation is the result of adsorption kinetics with oxygen penetrating the crystalline lattice much more readily than argon. The effective size of argon appears to be larger than oxygen, despite many references which assume oxygen to be a larger molecule. Inorganic crystalline adsorbents with the ability to clearly resolve oxygen and argon more rapidly and reproducibly than carbon molecular sieves could find widespread applications in oxygen purification and argon generation, especially in newer rapid cycle PSA processes.

ACKNOWLEDGEMENT

The authors thank Tony Haastrup, Christopher C.H. Lin and Gabor Konya for their contributions. Financial support is gratefully acknowledged from the Alberta Ingenuity Fund, Natural Sciences and Engineering Research Council of Canada Discovery Grant Program, US Department of Energy funding, and the NSERC Industrial Chair in New Molecular Sieves.

REFERENCES

1. Barrer, R.M.; Robins, A.B. (1953) Sorption of mixtures. Part 1 – Molecular sieve separations of permanent and inert gases. *Trans. Faraday Soc.*, *49*: 807.
2. Lard, E.W.; Horn, R.C. (1960) Separation and determination of argon, oxygen, and nitrogen by gas chromatography. *Anal. Chem.*, *32* (7): 878.
3. Goyette, B.; Vigneault, C.; Raghavan, G.S.V. (1994) Effect of argon on gas chromatographic analysis for controlled atmosphere storage. *Trans. ASAE*, *37*: 1221.
4. Sarma, V.V.S.S.; Abe, O.; Saino, T. (2003) Chromatographic separation of nitrogen, argon, and oxygen in dissolved air for determination of triple oxygen isotopes by dual-inlet mass spectrometry. *Anal. Chem.*, *75*: 4913.
5. Kovak, K.W.; Agrawal, R.; Peterson, J.C. (1992) Method of purifying argon through cryogenic adsorption. U.S. Patent 5,159,816, November 3, 1992.
6. Sebastian, J.; Jasra, R.V. (2005) Sorption of nitrogen, oxygen, and argon in silver-exchanged zeolites. *Ind. Eng. Chem. Res.*, *44*: 8014.

7. Walker, D.A.J. (1966) Chromatographic separation of argon and oxygen using molecular sieve. *Nature*, *209*: 197.
8. Karlsson, B.M. (1966) Heat treatment of molecular sieves for direct separation of argon and oxygen at room temperature by gas chromatography. *Anal. Chem.*, *38*: 668.
9. Maroulis, P.J.; Coe, C.G. (1989) Calcium chabazite adsorbent for the gas chromatographic separation of trace argon-oxygen mixtures. *Anal. Chem.*, *61*: 1112.
10. Pollock, G.E.; O'Hara, D.; Hollis, O.L. (1984) Gas chromatographic separation of nitrogen, oxygen, argon, and carbon monoxide using custom-made porous polymers from high purity divinylbenzene. *J. Chromatogr. Sci.*, *22*: 343.
11. Pollock, G.E. (1986) Synthesis of a further improved porous polymer for the separation of nitrogen oxygen, argon, and carbon monoxide by gas chromatography. *J. Chromatogr. Sci.*, *24*: 173.
12. Rege, S.U.; Yang, R.T. (2006) Kinetic separation of oxygen and argon using molecular sieve carbon. *Adsorption*, *6*: 15.
13. Jin, X.; Malek, A.; Farooq, S. (2006) Production of argon from an oxygen–argon mixture by pressure swing adsorption. *Ind. Eng. Chem. Res.*, *45*: 5775.
14. Ma, Y.H.; Sun, W.; Bhandakar, M.; Wang, J.; Miller, G.W. (1991) Adsorption and diffusion of nitrogen, oxygen, argon, and methane in molecular sieve carbon at elevated pressures. *Sep. Technology*, *1*: 90.
15. Reid, C.R.; O'koye, I.P.; Thomas, K.M. (1998) Adsorption of gases on carbon molecular sieves used for air separation. Spherical adsorptives as probes for kinetic selectivity. *Langmuir*, *14*: 2415.
16. Reid, C.R.; Thomas, K.M. (1999) Adsorption of gases on a carbon molecular sieve used for air separation: Linear adsorptives as probes for kinetic selectivity. *Langmuir*, *15*: 3206.
17. Kuznicki, S.M.; Bell, V.A.; Petrovic, I.; Blosser, P.W. (1999) Separation of nitrogen from mixtures thereof with methane utilizing barium exchanged ETS-4. U.S. Patent 5,989,316, November 23, 1999.
18. Kuznicki, S.M.; Bell, V.A.; Petrovic, I.; Desai, B.T. (2000) Small-pored crystalline titanium molecular sieve zeolites and their use in gas separation processes. U.S. Patent 6,068,682, May 30, 2000.
19. Kuznicki, S.M.; Bell, V.A.; Nair, S.; Hillhouse, H.W.; Jacubinas, R.M.; Braunbarth, C.M.; Toby, B.H.; Tsapatsis, M. (2001) A titanosilicate molecular sieve with adjustable pores for size-selective adsorption of molecules. *Nature*, *412*: 720.
20. Kuznicki, S.M.; Dang, D.; Hayhurst, D.T.; Thrush, K.A. (1994) Use of crystalline molecular sieves containing charged octahedral sites in removing volatile organic compounds from a mixture of the same. U.S. Patent 5,346,535, September 13, 1994.
21. Sebastián, V.; Lin, Z.; Rocha, J.; Téllez, C.; Santamaría, J.; Coronas, J. (2005) A new titanosilicate umbite membrane for the separation of H_2. *Chem. Commun.*, *24*: 3036.

22. Sebastián, V.; Lin, Z.; Rocha, J.; Téllez, C.; Santamaría, J.; Coronas, J. (2006) Synthesis, characterization, and separation properties of Sn- and Ti-silicate umbite membranes. *Chem. Mater.*, *18*: 2472.
23. Sandomirskii, P.A.; Belov, N.V. (1979) The OD structure of zorite. *Sov. Phys. Crystallogr.*, *24*: 686.
24. Philippou, A.; Anderson, M.W. (1996) Structural investigation of ETS-4. *Zeolites*, *16*: 98.
25. Cruciani, G.; De Luca, P.; Nastro, A.; Pattison, P. (1998) Rietveld refinement of the zorite structure of ETS-4 molecular sieves. *Micropor. Mesopor. Mater.*, *21*: 143.
26. Sawada, J.A.; Rode, E.J.; Kuznicki, S.M.; Lin, C.C.H. (2008) Silicate materials, method for their manufacture, and the method for using such silicate materials for adsorptive fluid separations. International Patent WO 2008/002463 A2, January 3, 2008.
27. Kuznicki, S.M. (1990) Preparation of small-pored crystalline titanium molecular sieve zeolites. U.S. Patent 4,938,939, July 3, 1990.
28. Breck, D.W. (1974) *Zeolite molecular sieves: structure, chemistry, and use*; John Wiley & Sons: New York.
29. Hirschfelder, J.O.; Curtiss, C.F.; Bird, B.R. (1964) *Molecular Theory of Gases and Liquids*; Corrected printing with notes added. John Wiley & Sons: New York.
30. Sircar, S.; Myers, A.L. (2003) *Gas Separation by Zeolites*, In: *Handbook of Zeolite Science and Technology*; Auerbach, S.M.; Carrado, K.A.; Dutta, P.K., eds.; Marcel Dekker: New York.
31. Kopelevich, D.I.; Chang, H.-C. (2001) Diffusion of inert gases in silica sodalite: Importance of lattice flexibility. *J. Chem. Phys.*, *115* (20): 9519.
32. Webster, C.E.; Drago, R.S.; Zerner, M.C. (1998) Molecular dimensions of adsorptives. *J. Amer. Chem. Soc.*, *120* (22): 5509.
33. Webster, C.E.; Drago, R.S.; Zerner, M.C. (1999) A method for characterizing effective pore sizes of catalysts. *J. Phys. Chem. B*, *103* (8): 1242.
34. Webster, C. E.; Cottone, A. III; Drago, R.S. (1999) Multiple equilibrium analysis description of adsorption on Na-mordenite and H-mordenite. *J. Amer. Chem. Soc.*, *121* (51): 12127.